# Hybrid Digital-Analog Transmission Taking Into Account D/A and A/D Conversion

Matthias Rüngeler and Peter Vary
Institute of Communication Systems and Data Processing ( ind )
RWTH Aachen University, Germany
{ruengeler | vary}@ind.rwth-aachen.de

***Abstract*—Efficient digital transmission of continuous-amplitude signals requires source coding which comes at the price of unavoidable quantization errors. Thus, even in clear channel conditions, the quality of the decoded signal is limited due to these source coding errors (quantization). Hybrid Digital-Analog (HDA) codes circumvent this limitation by additionally transmitting the source coding error with quasi-analog methods (discrete-time, quasi-continuous-amplitude) with neither increasing the total transmission power, nor the occupied frequency bandwidth on the radio channel. So far, for HDA transmission, the potential distortion additionally introduced by D/A and A/D conversion of the analog signal has not been considered. In this paper, the effect of clipping and limited resolution of this conversion on the performance of HDA transmission is evaluated. For random variables and speech signals, simulations verify that even with poor A/D and D/A conversion (3 bit resolution) the HDA concept outperforms conventional purely digital transmission systems at all channel qualities while additionally eliminating the quality limitation effect.**

***Index Terms*—Hybrid Digital-Analog (HDA), clipping and limited resolution of A/D and D/A converters**

## I. Introduction

Conventional digital transmission systems are based on the source-channel separation theorem. The digitized analog speech, audio, or video signal is processed by a source encoder which delivers a sequence of quantized source parameters. Thereafter, the bit stream of the source parameters is protected by a channel encoder. These systems are usually optimized for the expected worst-case channel condition. If a feedback channel is not available, adaptive multi rate (AMR) techniques cannot be implemented. Then, even if the receiver experiences a better channel quality (cSNR) the signal-to-noise ratio (pSNR) of the decoded source parameters saturates. This saturation is caused by the inherent errors introduced by the digital source encoder, even in the case of error-free transmission of the coded bits. The saturation effect can be circumvented by adding continuous-amplitude processing and transmission. With these Hybrid-Digital Analog (HDA) transmission systems, the transmission fidelity improves for increasing channel qualities without the need to adapt the coding scheme.

Skoglund et al. [1] have proposed a HDA system heavily relying on numerical optimizations and exhaustive search in the decoding algorithms. In [2], [3] a more efficient design for HDA transmission benefiting from the power and flexibility of conventional digital channel codes is presented. In the literature, the analog error symbols are distorted only by the noisy analog channel. Additionally, the analog signal is distorted by the unavoidable A/D and D/A conversion when using digital signal processing. This conversion usually comes with limited resolution and even clipping. This effect should not be neglected: For a compressing Archimedes spiral, an experimental evaluation with software defined radios showed a saturation of the quality at around $20\,\mathrm{dB}$ which is due to the 16 bit converters [4]. In this paper, the performance of HDA transmission with A/D and D/A converters with limited resolution and clipping is considered.

## II. Hybrid Digital-Analog Transmission and Purely Digital Transmission

Fig. 1 shows a conventional digital transmission system. The source vector $\boldsymbol{u}$ consists of $M$ continuous-amplitude and discrete-time symbols. It is source encoded with $F_{\mathrm{D}}$ bits per source symbol to in total $\ell_{\boldsymbol{v}_{\mathrm{D}}}$ source bits, yielding the bit vector $\boldsymbol{v}_{\mathrm{D}}$. Subsequently, a digital channel code followed by digital modulation transforms the source bits into $N$ real-valued symbols forming the channel input $\boldsymbol{y}_{\mathrm{D}}$. Here, channel coding and modulation is combined in one step (ccm), thus, the ratio between the number of bits $\ell_{\boldsymbol{v}_{\mathrm{D}}}$ and the number of real symbols $N$ is denoted by the coding-modulation rate $r_{\mathrm{D}}^{\mathrm{ccm}} = \frac{\ell_{\boldsymbol{v}_{\mathrm{D}}}}{N}$. When considering an AWGN channel, the noise vector $\boldsymbol{n}$ disturbs the channel symbols, thereby yielding the received symbols $\boldsymbol{z}_{\mathrm{D}}$. The channel signal to noise ratio is

$$\mathrm{cSNR} = \frac{\mathrm{E}\{||\boldsymbol{y}_{\mathrm{D}}||^2\}}{\mathrm{E}\{||\boldsymbol{n}||^2\}}. \qquad (1)$$

After demodulation, channel decoding, and reconstruction of quantized values, $\hat{\boldsymbol{u}}_{\mathrm{D}}$ gives an estimate of the initial source symbols $\boldsymbol{u}$.

Fig. 2 illustrates the corresponding HDA transmission system [2]. The general idea is to use a conventional digital transmission system for $\boldsymbol{u}$ and to additionally transmit the source coding error $\boldsymbol{u}_{\mathrm{H}}^{\mathrm{a}}$ by using continuous-amplitude (pseudo-analog) discrete-time processing. The upper branch of the hybrid encoder and decoder is referred to as the *digital* branch and the lower branch as the *analog* branch. All operations, also in the analog branch, are conducted by digital signal processing. The continuous-amplitude symbols are floating or fixed point variables with a precision depending on the digital processor. All variables in the figures are already digitized. Here, the necessary A/D and D/A conversion is assumed to have a sufficiently high quality to not affect the results. The digital branch is a purely digital transmission system with $D$ real channel per $M$ source symbols. The analog branch takes $A$channel uses. Thus, the number of channel uses per HDA frame is $N = D + A$ and the coding-modulation rate in the digital branch is $r_{\mathrm{H}}^{\mathrm{ccm}} = \frac{\ell_{\boldsymbol{v}_{\mathrm{H}}}}{N-A} = \frac{\ell_{\boldsymbol{v}_{\mathrm{H}}}}{D}$. In the

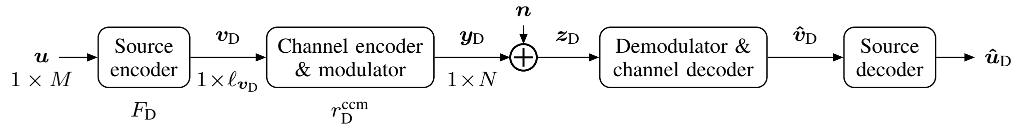


Fig. 1. Purely digital transmission system.

hybrid encoder, the source encoder converts $\boldsymbol{u}$ to the bit vector $\boldsymbol{v}_{\mathrm{H}}$ with $F_{\mathrm{H}}$ bits per source symbol. The source bis are decoded locally in the transmitter to $\boldsymbol{u}_{\mathrm{H}}^{\mathrm{d}}$ while the source coding error $\boldsymbol{u}_{\mathrm{H}}^{\mathrm{a}} = \boldsymbol{u} - \boldsymbol{u}_{\mathrm{H}}^{\mathrm{d}}$ is then transmitted via the analog branch. The analog mapper uses the continuous-amplitude function $\boldsymbol{y}_{\mathrm{H}}^{\mathrm{a}} = \boldsymbol{f}(\boldsymbol{u}_{\mathrm{H}}^{\mathrm{a}})$ to map the entries of $\boldsymbol{u}_{\mathrm{H}}^{\mathrm{a}}$ to the entries of $\boldsymbol{y}_{\mathrm{H}}^{\mathrm{a}}$ with length $A$ and average power $\frac{1}{A}\,\mathrm{E}\{||\boldsymbol{y}_{\mathrm{H}}^{\mathrm{a}}||^2\} = 1$. The ratio between the input and the output dimensions of the block is $r_{\mathrm{H}}^{\mathrm{mapp}} = \frac{M}{A}$. This mapping $\boldsymbol{f}(\cdot)$ could, e.g., be a linear amplification or a nonlinear function with a rate of $r_{\mathrm{H}}^{\mathrm{mapp}} = 1$ or in case of a mapping yielding one complex symbol for one real input symbol $r_{\mathrm{H}}^{\mathrm{mapp}} = \frac{1}{2}$. After multiplexing the symbols from the digital and the analog branch and transmission over the AWGN channel, the received symbols are demultiplexed and conveyed to the digital and analog decoding branches. The analog demapper then gives $\hat{\boldsymbol{u}}_{\mathrm{H}}^{\mathrm{a}}$ as the estimate of $\boldsymbol{u}_{\mathrm{H}}^{\mathrm{a}}$ which can be facilitated using several alternative methods such as maximum likelihood (ML), minimum mean square error (MMSE) and linear minimum mean square error (LMMSE) estimators. The ML estimator applies the inverse function of $\boldsymbol{f}(\cdot)$ whereas the LMMSE estimator additionally weights the received symbols with $\frac{\mathrm{cSNR}}{(1+\mathrm{cSNR})}$ before applying the inverse function of $\boldsymbol{f}(\cdot)$ [5]. In this paper, a linear analog mapper and LMMSE estimation is employed. The outputs of the analog and digital branches are added, whereby $\hat{\boldsymbol{u}}_{\mathrm{H}}$ gives an estimate of the initial source symbols. Finally, the end-to-end parameter signal to noise ratio for both systems is described by

$$\mathrm{pSNR} = \frac{\mathrm{E}\{||\boldsymbol{u}||^2\}}{\mathrm{E}\{||\boldsymbol{u} - \hat{\boldsymbol{u}}||^2\}}. \tag{2}$$

For a fair comparison between the purely digital and the HDA transmission systems, the transmission power as well as the number of channel uses $N$ must be equal. Thus, the number of channel uses $D$ for the digital branch has to be lowered to $D = N - A$. This can be achieved by lowering the bit rate of the source encoder in the HDA system. Then fewer bits need to be protected against channel noise and thus the same or even stronger channel coding can be applied ($r_{\mathrm{D}}^{\mathrm{ccm}} \geq r_{\mathrm{H}}^{\mathrm{ccm}}$) as in the purely digital case. However, the bit rate of the HDA system cannot be lowered too much, since then the loss in pSNR due to coarser quantization cannot be compensated anymore by the analog branch. In [2], it is stated by how much the bit rate can be lowered to design a superior HDA system for any purely digital system. If additionally an LMMSE estimator is used as the analog demapper, the performance of the HDA system is superior or equal to the purely digital transmission system at *all channel qualities* for AWGN and even fading channels [2]. Especially in the context of unknown radio channel qualities, or with channel qualities which may be higher than expected while designing the system, the HDA system exhibits the very desirable property to increase the end-to-end pSNR with rising channel qualities.

## III. D/A and A/D Conversion in Analog Branch

In Fig. 2, it is assumed that the interface to the real world (the actual source samples and the channel symbols) is perfect and no additional distortion is introduced. For a real-world system (Fig. 3), the effect of D/A and A/D conversion also have to be considered. The captured analog (discrete-time, continuous-amplitude) input signal $\tilde{\boldsymbol{u}}$ has to be converted (quantizer ①) to the digital domain ($\boldsymbol{u}$) before further processing. Also the analog symbols $\boldsymbol{y}_{\mathrm{H}}^{\mathrm{a}}$ ② and the potentially non-binary modulation symbols $\boldsymbol{y}_{\mathrm{H}}^{\mathrm{d}}$ ④ of the HDA encoder are passed through a D/A convertor at the transmitter ($\tilde{\boldsymbol{y}}_{\mathrm{H}}^{\mathrm{a}}$ and $\tilde{\boldsymbol{y}}_{\mathrm{H}}^{\mathrm{d}}$) and also the receiver employs A/D converters (⑤ & ③). The impact of the A/D ② and D/A ③ conversion in the analog branch, which are boxed with a bold line, are considered here. The other A/D and D/A converters also appear in a purely digital transmission system and do, if properly designed, not impact the performance difference between purely digital and HDA transmission. The A/D and D/A converters (② & ③) are modeled by a symmetric *uniform* mid-rise quantizer. Two parameters are relevant: First, $F_{\mathrm{TX}}$ and $F_{\mathrm{RX}}$ define the number of bits of the quantizers at the transmitter and the receiver, respectively. Second, the range of the quantizer is relevant ($(-C_{\mathrm{TX}}, C_{\mathrm{TX}})$ and $(-C_{\mathrm{RX}}, C_{\mathrm{RX}})$). The reconstruction values of the uniform quantizers are in this range and all values with greater absolute value are clipped.

### *A. D/A ② at Transmitter*

The aim of the parametrization of the D/A converter ② at the transmitter is to minimize the introduced distortion. There

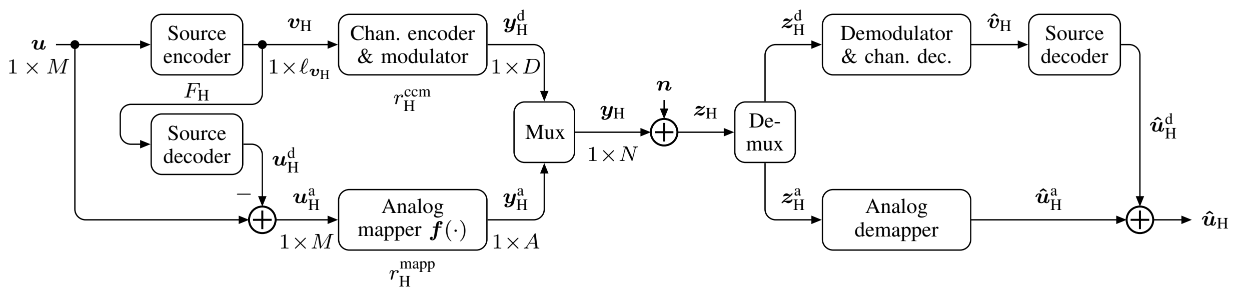


Fig. 2. HDA transmission system without consideration of D/A and A/D conversion.

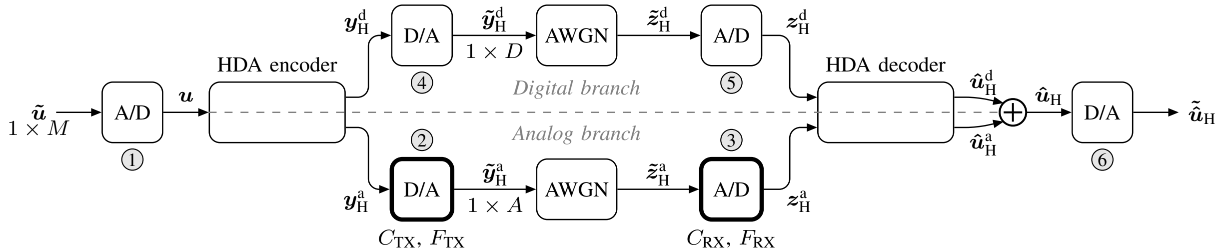


Fig. 3. HDA transmission system with A/D and D/A conversion. The properties of D/A and A/D conversion in the analog branch are considered. The variables $C_{\mathrm{TX}}$ and $C_{\mathrm{RX}}$ describe the maximum range of the quantization and $F_{\mathrm{TX}}$ and $F_{\mathrm{RX}}$ the number of bits of the uniform quantizers.

are two effects which are considered here. First the distortion $\mathrm{MSE_C}$ introduced by the limited range ($C_{\mathrm{TX}}$) of the quantizer, i.e., the clipping, and second the distortion $\mathrm{MSE_Q}$ introduced by quantization noise. For a given clipping level $C_{\mathrm{TX}}$ and the number of bits $F_{\mathrm{TX}}$ of the quantizer, the number of quantization levels is $L = 2^{F_{\mathrm{TX}}}$, the step height of the uniform quantizer is $h = \frac{2 \cdot C_{\mathrm{TX}}}{L}$ and the reconstruction value with the largest value is given as $m = C_{\mathrm{TX}} - \frac{1}{2} \cdot h = C_{\mathrm{TX}} \cdot \left(1 - \frac{1}{L}\right)$. All values outside of $(-C_{\mathrm{TX}}, C_{\mathrm{TX}})$ are mapped to the greatest/smallest reconstruction value $\pm m$ of the quantizer. Thus, with the pdf $\mathrm{p}(y_{\mathrm{H}}^{\mathrm{a}})$ of the entries $y_{\mathrm{H}}^{\mathrm{a}}$ of the vector $\boldsymbol{y}_{\mathrm{H}}^{\mathrm{a}}$ to be transmitted, the influence of clipping is calculated as [6]:

$$\mathrm{MSE_C} = \int_{C_{\mathrm{TX}}}^{\infty} (y_{\mathrm{H}}^{\mathrm{a}} - m)^2 \, \mathrm{p}(y_{\mathrm{H}}^{\mathrm{a}}) \, \mathrm{d}y_{\mathrm{H}}^{\mathrm{a}} + \int_{-\infty}^{-C_{\mathrm{TX}}} (y_{\mathrm{H}}^{\mathrm{a}} + m)^2 \, \mathrm{p}(y_{\mathrm{H}}^{\mathrm{a}}) \, \mathrm{d}y_{\mathrm{H}}^{\mathrm{a}}.$$

Values within the range are mapped to the nearest reconstruction value of the quantizer. The introduced distortion $\mathrm{MSE_Q}$ by quantization is:

$$\mathrm{MSE_Q} = \sum_{i=1}^{L} \int_{-C_{\mathrm{TX}} + (i-1) \cdot h}^{-C_{\mathrm{TX}} + i \cdot h} \left( y_{\mathrm{H}}^{\mathrm{a}} - C_{\mathrm{TX}} \left( \frac{2i-1}{L} - 1 \right) \right)^2 \mathrm{p}(y_{\mathrm{H}}^{\mathrm{a}}) \, \mathrm{d}y_{\mathrm{H}}^{\mathrm{a}}.$$

The overall introduced distortion $\mathrm{MSE_{TX,HW}} = \mathrm{MSE_Q} + \mathrm{MSE_C}$ is the sum of both effects. For a given pdf $\mathrm{p}(y_{\mathrm{H}}^{\mathrm{a}})$ and a given number of quantization bits $F_{\mathrm{TX}}$, the clipping value $C_{\mathrm{TX}}$ minimizing $\mathrm{MSE_{TX,HW}}$ has to be found. Greater values lead to a smaller distortion due to clipping, but the step height $h$ of the quantizer grows. Thus, the distortion due to quantization increases. Smaller values decrease the quantization noise, but increase the impact of clipping. The optimal value is a tradeoff which has to be found numerically for a given $F_{\mathrm{TX}}$ and $\mathrm{p}(y_{\mathrm{H}}^{\mathrm{a}})$.

If, as a simple example, the source samples $\tilde{\boldsymbol{u}}$ follow a uniform distribution and as source encoding, uniform quantization is used, the pdf $\mathrm{p}(y_{\mathrm{H}}^{\mathrm{a}})$ of the analog output of the HDA encoder also follows a uniform distribution. After the analog mapper (Fig. 2), the average power $\frac{1}{A}\,\mathrm{E}\{||\boldsymbol{y}_{\mathrm{H}}^{\mathrm{a}}||^2\}$ is 1 and thus its range is $(-\sqrt{3}, \sqrt{3})$. The numerical optimization of the clipping value yields $C_{\mathrm{TX}} = \sqrt{3}$ which is at the same time the smallest possible value without clipping.

For Gaussian source symbols and Lloyd-Max quantization in the HDA encoder, the pdf of $y_{\mathrm{H}}^{\mathrm{a}}$ is not uniform anymore. Then, the optimal $C_{\mathrm{TX}}$ has to be found numerically. For all permutations of the number of bits $F_{\mathrm{H}}$ per source symbol in the HDA encoder and the word length $F_{\mathrm{TX}}$ of the D/A converter in the transmitter, the optimal clipping values $C_{\mathrm{TX}}$ are stated in Table I. For rising $F_{\mathrm{TX}}$, the quantization noise $\mathrm{MSE_Q}$ decreases and due to the above described tradeoff, the clipping value has to be increased. This is reflected in the table. A change of $F_{\mathrm{H}}$ leads to different pdfs $\mathrm{p}(u_{\mathrm{H}}^{\mathrm{a}})$ of the analog output of the HDA encoder which also affects the optimal $C_{\mathrm{TX}}$.

| $F_{\mathrm{H}}\downarrow \backslash F_{\mathrm{TX}}\rightarrow$ | **1** | **2** | **3** | **4** | **5** | **6** | **7** | **8** |
|---|---|---|---|---|---|---|---|---|
| **1** | 1.60 | 1.87 | 2.83 | 3.09 | 3.71 | 4.32 | 4.77 | 5.18 |
| **2** | 1.61 | 1.76 | 3.18 | 3.78 | 4.56 | 5.60 | 6.63 | 7.38 |
| **3** | 1.61 | 1.73 | 3.05 | 4.31 | 5.80 | 7.46 | 8.88 | 10.39 |
| **4** | 1.61 | 1.73 | 2.85 | 3.99 | 6.28 | 9.16 | 12.04 | 14.66 |
| **5** | 1.61 | 1.73 | 2.86 | 3.93 | 5.81 | 9.74 | 14.61 | 19.48 |
| **6** | 1.61 | 1.74 | 2.85 | 3.89 | 5.71 | 8.92 | 14.87 | 21.83 |
| **7** | 1.61 | 1.74 | 2.86 | 3.90 | 5.78 | 8.87 | 12.91 | 19.36 |
| **8** | 1.61 | 1.74 | 2.87 | 3.92 | 5.80 | 9.00 | 12.77 | 17.62 |

TABLE I
OPTIMAL $C_{\mathrm{TX}}$ FOR D/A CONVERSION IN ANALOG BRANCH FOR GAUSSIAN SOURCE SYMBOLS QUANTIZED WITH $F_{\mathrm{H}}$ BITS IN HDA ENCODER.

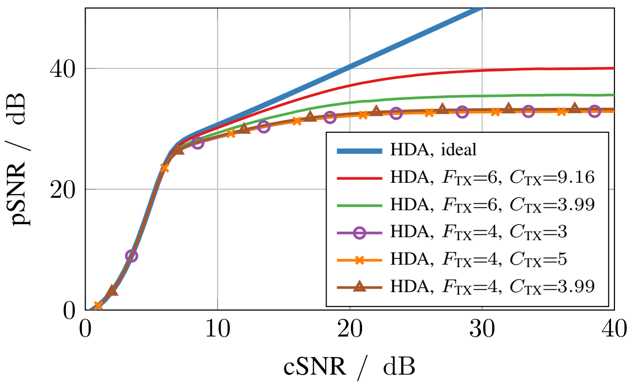


Fig. 4. HDA transmission with different D/A converters ② in the transmitter, an ideal A/D converter ③ in the receiver, and a Gaussian source with $F_{\mathrm{H}}$=4.

To assess the performance of the HDA transmission system, monte carlo simulations with a source block length of $M = 80$ are conducted. First, for Gaussian source symbols, the source encoder is a Lloyd-Max quantizer (LMQ). Here, $F_{\mathrm{D}} = 5$ bits are used in the purely digital case, while for the HDA case the quantizer in the source coder employs one bit less ($F_{\mathrm{H}} = 4$). The output bits of the source encoder are channel encoded using convolutional coding with a rate-$\frac{1}{2}$ recursive systematic convolutional code with the generator polynomial $\{1, 15/13\}_8$ — the same code which is used as a component code in the UMTS-LTE Turbo code. Then, BPSK modulation is employed. To guarantee a fair comparison between all systems, puncturing is applied to the codewords to always yield $N = 560$ channel uses. In the HDA case, $D = 480$ channel uses are allocated to the digital branch and $A = M = 80$ channel uses to the analog branch. Figure 4 shows the simulation results for different converters at the transmitter for Gaussian source symbols. The curve labeled “HDA, ideal” does not consider any distortion introduced by D/A or A/D conversion in the analog branch. The other curves employ an ideal A/D converter at the receiver but consider the distortion at the transmitter. For $F_{\mathrm{TX}} = 4$ the optimal clipping value is $C_{\mathrm{TX}} = 3.99$. Varying the value to higher $C_{\mathrm{TX}} = 5$ or lower $C_{\mathrm{TX}} = 3$ values just slightly decreases the performance. For $F_{\mathrm{TX}} = 6$, a different $C_{\mathrm{TX}} = 9.16$ is chosen which leads to an improved performance. Choosing the value which was optimal for the lower word length ($C_{\mathrm{TX}} = 3.99$) drastically decreases the performance. Thus, the A/D should be parametrized wisely.

For very low word lengths, i.e., $F_{\mathrm{TX}} = 1$ another effect arises. Since the reconstruction values of the quantizers are $\pm\frac{1.61}{2} \approx 0.80$, the power of the transmitted values $\tilde{y}^{\mathrm{a}}_{\mathrm{H}}$ is lower than the targeted power of 1 by $1.9\,\mathrm{dB}$. Thus, for a fair comparison, the power should be increased by this value which would lead to an improvement of the performance in pSNR of at least $1.9\,\mathrm{dB}$ with LMMSE estimation. Since for increasing word lengths, e.g., for $F_{\mathrm{TX}} = 4$, this loss decreases to just $0.22\,\mathrm{dB}$, this loss is not compensated in the simulations.

### *B. A/D ③ at Receiver*

The aim at the receiver is to minimize the overall distortion introduced by both, the D/A and the A/D converter. Thus, not the received symbols have to be captured as good as possible, but the output of the receiver A/D converter should describe the sent reconstruction levels of the quantizer as close as possible. The analogy to a digital demodulation system is quite close. At best, the receiver A/D converter denoises the sent reconstruction levels. This can be achieved by using the same parametrization at the receiver as in the transmitter, especially when using the same clipping values ($C_{\mathrm{RX}} = C_{\mathrm{TX}}$). In [7] it is shown by information theoretic means, that is is sufficient to use the same number of quantization levels at the receiver as discrete levels at the transmitter to achieve capacity.

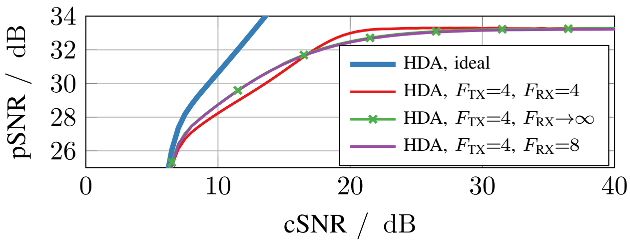


Fig. 5. HDA transmission with a fixed D/A converter at the transmitter ② with different A/D converters ③ at the receiver. Gaussian source pdf, $F_{\mathrm{H}}$=4, $C_{\mathrm{RX}}$=$C_{\mathrm{TX}}$=3.99.

Figure 5 shows simulation results with one fixed D/A converter at the transmitter and different A/D converters at the receiver. The receivers use the same clipping values as the transmitter ($C_{\mathrm{RX}} = C_{\mathrm{TX}}$), but the word length is varied. The system with the same word length ($F_{\mathrm{RX}} = F_{\mathrm{TX}} = 4$) achieves the best performance, especially for channel qualities just below the saturation of the system (cSNR $\approx 25\,\mathrm{dB}$). Here, noisy symbols are mapped to the exact sent values. Systems with a higher world length ($F_{\mathrm{RX}} = 8$) or even without any distortion by the receiver show an equal performance which is slightly better at lower channel qualities (cSNR $\approx 13\,\mathrm{dB}$). But they cannot denoise the received symbols at cSNR $\approx 25\,\mathrm{dB}$ and thus exhibit a big performance gap to $F_{\mathrm{RX}} = 4$.

In case of $F_{\mathrm{RX}} = F_{\mathrm{TX}}$, the pdf of the effective noise $z^{\mathrm{a}}_{\mathrm{H}} - y^{\mathrm{a}}_{\mathrm{H}}$ is a convolution between the quantization noise of the D/A at the transmitter, which is uniform, and a series of diracs which emerge when choosing the wrong quantization level from the noisy received symbols. For a small channel noise power, the quantization levels are correct and thus, just the quantization noise remains. In case of an “ideal” receiver, the uniform quantization noise is convolved with the Gaussian channel noise pdf. For small channel noise powers, the result is always greater than for $F_{\mathrm{RX}} = F_{\mathrm{TX}}$, but for higher channel noise powers (cSNR $\gtrapprox 18\,\mathrm{dB}$) the diracs have a greater power than the channel noise.

## IV. Simulation Results

### *A. Source Coding by Scalar Quantization*

Figure 6 shows the performance of purely digital and HDA transmission systems with source symbols following a uniform pdf. The transmitter D/A and receiver A/D converters are designed with the same parameters ($C_{\mathrm{RX}} = C_{\mathrm{TX}}$, $F_{\mathrm{RX}} = F_{\mathrm{TX}}$). With all configurations, the performance of the HDA system increases with rising channel qualities until a certain maximum pSNR is reached. This limit rises with higher word lengths of the converters obeying the 6dB-per-bit rule, i.e., for a quantizer with one bit more, the limit increases by $6\,\mathrm{dB}$. This means that already with $F_{\mathrm{TX}} = 2$, the performance of a purely digital system is superseded by HDA transmission. A linear transmission system with LMMSE estimation and D/A and A/D conversion is shown for comparison which exhibits generally a lower performance and saturates at $36\,\mathrm{dB}$ due to the 6 bit quantizers.

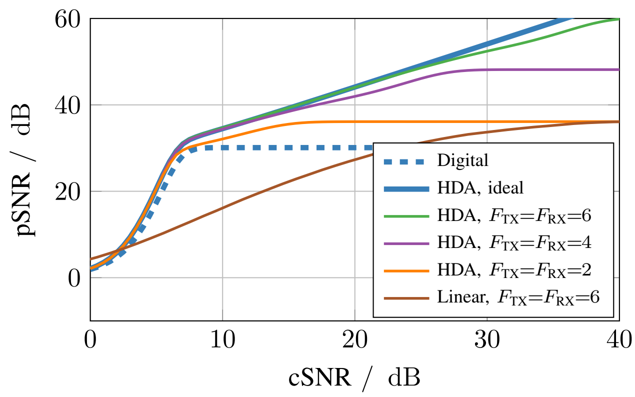


Fig. 6. HDA and purely digital transmission for a uniform source pdf. The D/A and A/D conversion in the transmitter ② and receiver ③ in the analog branch have the same design: $C_{\mathrm{RX}}$=$C_{\mathrm{TX}}$=$\sqrt{3}$, $F_{\mathrm{RX}}$=$F_{\mathrm{TX}}$, $F_{\mathrm{H}}$=4, $F_{\mathrm{D}}$=5. Purely linear system with LMMSE estimation and D/A and A/D conversion for comparison.

Figure 7 shows the same behavior for Gaussian source symbols. Also here, for rising channel qualities, the pSNR increases until a certain limit. Here, the 6dB-per-bit rule is not obeyed. An increase from $F_{\mathrm{TX}} = 6$ to 8 bits leads to a gain of just $8\,\mathrm{dB}$ instead of $12\,\mathrm{dB}$. When using a converter with a higher word length, the range, i.e, the clipping value $C_{\mathrm{TX}}$ also has to be increased which reduces the gain. A

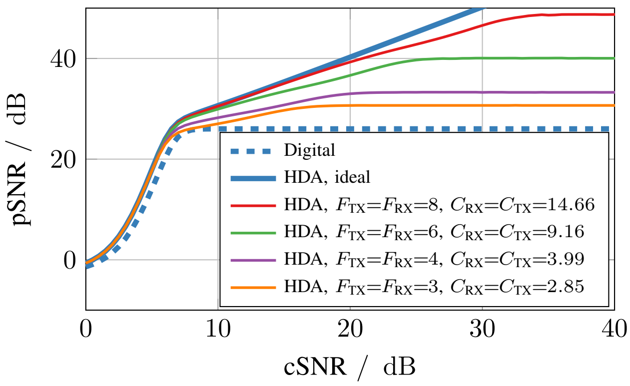


Fig. 7. HDA and purely digital transmission for a Gaussian source pdf. $C_{RX}$=$C_{TX}$, $F_{RX}$=$F_{TX}$, $F_H$=4, $F_D$=5.

future improvement could be a nonlinear preprocessing prior to the transmission via the analog branch to suffer less from distortion due to clipping.

### *B. Source Coding by ADPCM Speech Coding*

In Fig. 8 a lattice ADPCM speech coder [8] is employed. The speech signal are 96 sentences from the NTT database (16 kHz sampling rate) in "English" which sum up to a total duration of 12 minutes and 48 seconds. The same block lengths and channel encoding parameters as in the previous simulations are employed. The only change to the system depicted in Fig. 2 is in the analog mapper. Here, since the statistics of the speech signal is unknown a-priori, for each frame a power normalization factor is calculated, digitized and multiplexed with the output bits of the speech encoder to be transmitted via the digital branch. The optimal clipping values are chosen according to the pdf of $y_H^a$. Also for this system employing real-world speech signals and speech encoding, HDA transmission is superior to purely digital transmission. A resolution of only 3 bits for the D/A and A/D conversion in the analog branch suffices to achieve a superior performance which can be further increased with conversion with more bits.

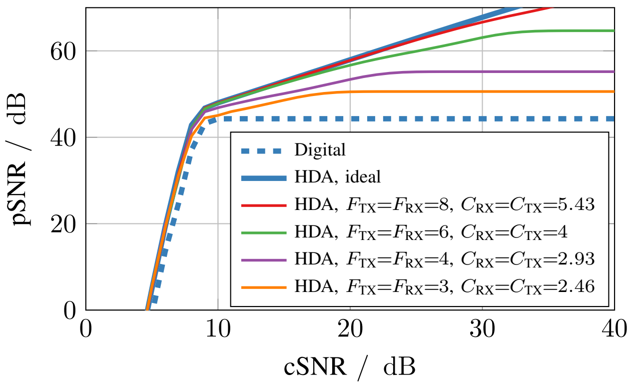


Fig. 8. HDA and purely digital transmission for speech using a lattice ADPCM speech coder [8]. $C_{RX}$=$C_{TX}$, $F_{RX}$=$F_{TX}$, $F_H$=4, $F_D$=5.

Nevertheless, the requirements for D/A and A/D conversion to achieve great performance of the analog branch of the HDA systems are comparatively low. D/A and A/D conversion with just 8 bit lead to a performance gain of 42 dB in pSNR in case of source symbols with a uniform pdf, to 22 dB in case of a Gaussian source and to 31 dB in case of speech coding. The overall pSNR of the HDA system is the sum of the performance of the digital branch and the analog branch. Thus, Hybrid Digital-Analog transmission enables high pSNRs since the basis is laid with a digital system and the performance of the analog branch is *on top*. This is an outstanding property compared to systems which only rely on continuous-amplitude transmission as, e.g., analog modulo block codes [9] or Archimedes spirals [4], [10]. All in all, it can be shown that the results in [2] also hold for HDA systems with D/A and A/D conversion, as long as their word lengths are above $F_{TX} \geq 3$. Thus, also with D/A and A/D conversion with limited resolution in the analog branch, HDA systems can be designed which exhibit a superior performance than purely digital transmission for all channel qualities.

## V. Conclusion

In this contribution, Hybrid Digital-Analog transmission with D/A and A/D conversion in the analog branch is considered. Their impact on the overall performance is elaborated and it is shown how to optimally parametrize them. Simulations are conducted for random variables with uniform and Gaussian pdf employing scalar quantization as source coding, as well as lattice ADPCM speech coding for speech signals. Even for conversion with just 3 bits, the HDA systems always exhibit a better performance than purely digital transmission for all channel qualities and therefore the design rules in [2] still hold. The big advantage of HDA transmission over systems with only continuous-amplitude transmission is that the performance of the analog branch is added *on top* to the performance of the digital branch. Thus, very high overall pSNR values can be reached.

## References


[1] M. Skoglund, N. Phamdo, and F. Alajaji, "Design and Performance of VQ-based Hybrid Digital-Analog Joint Source-Channel Codes," *IEEE Transactions on Information Theory*, vol. 48, no. 3, Mar. 2002.

[2] M. Rüngeler, J. Bunte, and P. Vary, "Design and Evaluation of Hybrid Digital-Analog Transmission Outperforming Purely Digital Concepts," *Communications, IEEE Transactions on*, vol. 62, no. 11, Nov 2014.

[3] M. Rüngeler and P. Vary, "Hybrid Digital Analog Transform Coding," in *2013 IEEE International Conference on Acoustics, Speech and Signal Processing (ICASSP)*. Vancouver: IEEE, May 2013.

[4] J. Garcia-Naya, O. Fresnedo, F. Vazquez-Araujo, M. Gonzalez-Lopez, L. Castedo, and J. Garcia-Frias, "Experimental evaluation of analog joint source-channel coding in indoor environments," in *Communications (ICC), 2011 IEEE International Conference on*, June 2011.

[5] O. Fresnedo, F. Vazquez-Araujo, L. Castedo, and J. Garcia-Frias, "Low-Complexity Near-Optimal Decoding for Analog Joint Source Channel Coding Using Space-Filling Curves," *IEEE Communications Letters*, vol. 17, no. 4, 2013.

[6] P. Vary and R. Martin, *Digital Speech Transmission - Enhancement, Coding & Error Concealment*. Wiley, Jan. 2006.

[7] J. Singh, O. Dabeer, and U. Madhow, "On the limits of communication with low-precision analog-to-digital conversion at the receiver," *Communications, IEEE Transactions on*, vol. 57, no. 12, Dec. 2009.

[8] M. Dietrich, "Performance and implementation of a robust ADPCM algorithm for wideband speech coding with 64 kbit/s," in *Proc. of Intl. Zürich Seminar on Digital Communications*, Zürich, Switzerland, 1984.

[9] T. Schmitz, M. Rüngeler, and P. Vary, "Analysis of analog modulo block codes," in *Proceedings of International ITG Conference on Systems, Communications and Coding (SCC)*. IEEE, Feb. 2015.

[10] P. Floor and T. Ramstad, "Noise Analysis for Dimension Expanding Mappings in Source-Channel Coding," *IEEE 7th Workshop on Signal Processing Advances in Wireless Communications, 2006. SPAWC 2006.*